Identification of a natural beige adipose depot in mice

Received for publication, November 23, 2018, and in revised form, February 15, 2019 Published, Papers in Press, March 1, 2019, DOI 10.1074/jbc.RA118.006838

Michelle Chan[‡§1], **Yen Ching Lim**[¶1], **Jing Yang**[‡‖], **Maria Namwanje**[‡], **Longhua Liu**[‡], and **Li Qiang**[‡2]

From the [‡]*Naomi Berrie Diabetes Center, Department of Pathology and Cell Biology, College of Physicians and Surgeons, Columbia University, New York, New York 10032, the* [§]*Department of Biological Sciences, Columbia University, New York, New York 10027, the* [¶]*Cardiovascular and Metabolic Disorders Program, Duke-NUS Medical School, Singapore 169857, Singapore, and the* [‖]*Department of Endocrinology, The First Affiliated Hospital of Xi'an Jiao Tong University, Xi'an City, Shaanxi Province, China*

Edited by Qi-Qun Tang

Beige fat is a potential therapeutic target for obesity and other metabolic diseases due to its inducible brown fat-like functions. Inguinal white adipose tissue (iWAT) can undergo robust brown remodeling with appropriate stimuli and is therefore widely considered as a representative beige fat depot. However, adipose tissues residing in different anatomic depots exhibit a broad range of plasticity, raising the possibility that better beige fat depots with greater plasticity may exist. Here we identified and characterized a novel, naturally-existing beige fat depot, thigh adipose tissue (tAT). Unlike classic WATs, tAT maintains beige fat morphology at room temperature, whereas high-fat diet (HFD) feeding or aging promotes the development of typical WAT features, namely unilocular adipocytes. The brown adipocyte gene expression in tAT is consistently higher than in iWAT under cold exposure, HFD feeding, and rosiglitazone treatment conditions. Our molecular profiling by RNA-Seq revealed up-regulation of energy expenditure pathways and repressed inflammation in tAT relative to eWAT and iWAT. Furthermore, we demonstrated that the master fatty acid oxidation regulator peroxisome proliferator-activated receptor α is dispensable for maintaining and activating the beige character of tAT. Therefore, we have identified tAT as a natural beige adipose depot in mice with a unique molecular profile that does not require peroxisome proliferator-activated receptor α.

The growing epidemics of obesity and its associated metabolic disorders such as type 2 diabetes have spurred much interest in the characterization of adipose tissue depots and their functional roles in the human body. Adipocytes have been classified into three distinct categories: white, brown, and, most recently, beige adipocytes. White adipocytes specialize in energy storage in the form of triglycerides, which can undergo lipolysis and release free fatty acids into circulation when needed (1). Additionally, white adipose tissue (WAT)[3] plays crucial roles in the maintenance of glucose and energy homeostasis through its endocrine functions (2, 3). In contrast, brown adipocytes oxidize endogenous triglycerides to generate heat, a process known as nonshivering thermogenesis. This process is accomplished primarily through the action of uncoupling protein 1 (UCP1), an inner mitochondrial membrane protein that uncouples electron transport from ATP synthesis by allowing inter-membrane protons to leak back into the mitochondrial matrix (4). This enables active substrate oxidation and reduced ATP production, with the generation of heat instead.

Emerging evidence has indicated that mammalian nonshivering thermogenesis is performed not only by classical brown adipocytes but also by brown-like white fat cells termed beige adipocytes (5, 6). These thermogenic adipocytes are interspersed within WAT depots and respond to environmental stimuli. Specifically, cold exposure, chronic endurance exercise, and β_3-adrenergic receptor activation in mice efficiently induce certain WAT depots to adopt features of brown adipose tissue (BAT), a process known as brown remodeling, browning, or beiging (7–10). Like classical brown adipocytes, beige adipocytes possess multilocular lipid droplets and densely-packed mitochondria that express *Ucp1* and other genes that promote energy expenditure (11, 12). The origin of beige cells has been explained by either trans-differentiation, the direct conversion of white adipocytes into brown-like cells (13, 14), or the *de novo* differentiation of unique beige precursors resident within WAT (15). Along with the development of thermogenic capacity during brown remodeling, stimulation of beige adipocyte activity has been associated with reduced body weight, insulin resistance, and adiposity (12, 16). As such, increasing the number or activity of thermogenic adipocytes in humans may have similar metabolic benefits. In adult humans, thermogenic adipocytes in the form of BAT has been discovered in multiple locations, including the axillary, cervical, supraclavicular, paravertebral, and abdominal subcutaneous regions (17). Transcriptional analyses of these adipose depots, however, indicate that nearly all human BAT expresses molecular markers selective to beige adipocytes in mice and do not express canonical

This work was supported by National Institutes of Health Grants R00DK97455 (to L. Q.) and R01DK112943 (to L. Q.), and Pilot and Feasibility Center Grant P30DK063608 (to L. Q.). The authors declare that they have no conflicts of interest with the contents of this article. The content is solely the responsibility of the authors and does not necessarily represent the official views of the National Institutes of Health.

This article contains Tables S1 and S2 and Figs. S1–S5.

The RNA-seq data are deposited in NCBI's Gene Expression Omnibus database under accession number GEO GSE123511.

[1] Both authors contributed equally to this article.

[2] To whom correspondence should be addressed. E-mail: lq2123@cumc.columbia.edu.

[3] The abbreviations used are: WAT, white adipose tissue; iWAT, inguinal white adipose tissue; UCP1, uncoupling protein 1; BAT, brown adipose tissue; tAT, thigh adipose tissue; HFD, high-fat diet; TZD, thiazolidinedione; qPCR, quantitative PCR; PPAR, peroxisome proliferator-activated receptor; DIO, diet-induced obesity; DEG, differentially expressed protein-coding genes; SVF, stromal vascular fraction; FPKM, fragments/kilobase of transcript/million mapped reads.

brown fat-selective genes (18, 19). Furthermore, the isolation of clonally derived beige-like adipocytes from adult humans has demonstrated the existence of beige adipocytes in human WAT (20). Browning has thus gained much attention as a potential therapeutic target in the treatment of obesity and other metabolic disorders (21, 22).

It is thus of great interest to understand the molecular mechanisms behind the regulation of WAT browning during which beige adipocytes are activated from basal status, as such knowledge would potentially allow for the manipulation of adipose plasticity and the improvement of metabolic health. Because iWAT is enriched with beige adipocytes and undergoes significant brown remodeling in response to genetic, pharmacological, and environmental stimuli (23), it is widely used as a source of these adipocytes to study their development as well as the process of WAT browning. However, numerous adipose depots exist in a variety of anatomic locations and exhibit a broad range of metabolic activity (24). This engenders the possibility that other fat depots may have higher browning capacities than iWAT and may serve as alternative or even superior beige fat sources. In our study, we identified an adipose depot in mice, adjacent to iWAT and attached to the thigh, which possesses higher browning potential than iWAT and expresses BAT-selective markers even without environmental stimuli; this fat depot may therefore serve as a more appropriate model for brown remodeling studies.

Results

Thigh adipose tissue is hyperplastic and has remarkable browning capability

Subcutaneous fat, particularly the inguinal depot, is widely used to study brown remodeling of white fat. However, even after significant brown remodeling, such as by cold exposure, its relative expression of brown adipocyte markers is still much lower than that of the canonical BAT. We therefore sought to identify a depot with higher browning potential, with the goal of establishing a better model for the investigation of adipose plasticity. We first noticed a small fat pad located toward the dorsal end of inguinal fat that was darker in color (Fig. 1*A*, *top panel*). Anatomically, this depot does not belong to any of the three divisions of iWAT (dorsolumbar, inguinal, and gluteal) (25, 26); it attaches to the thigh, and thus we named it thigh adipose tissue (tAT).

tAT exhibited high plasticity, as cold exposure induced the development of a nearly identical BAT-like morphology, whereas high-fat diet (HFD) feeding promoted its shift to a larger, lipid-filled white depot (Fig. 1*A*). These observations were corroborated with H&E staining of fat depots obtained from each treatment group (Fig. 1*B*). Under room temperature conditions, brown-like adipocytes were already present in tAT, in contrast to the white adipocyte morphology of iWAT. Upon cold exposure, iWAT exhibited the characteristic features of brown remodeling, as manifested through the development of numerous multilocular brown-like cells. Notably, the brown remodeling of tAT was much stronger than that of iWAT, because the majority of its cells adopted brown-like features. Moreover, unlike the authentic brown adipocytes, these cold-induced brown-like adipocytes in tAT were larger and more spherical, implying a WAT origin. This was supported by the fully-white adipocyte look of tAT in HFD or aged mice, namely the appearance of large, unilocular cells similar to adipocytes in iWAT (Fig. 1*B*). Collectively, these observations demonstrate that tAT is a hyperplastic fat depot.

Like BAT, tAT was responsive to cold exposure as observed by the induction of Ucp1 (Fig. 1*C*). To further characterize the browning potential of tAT, we compared its gene expression levels of brown markers and thermogenic regulators to those of a few other major fat depots including eWAT, the representative white fat; iWAT, a widely-used beige depot; and BAT, the classic brown fat, after chronic cold exposure. The expression of brown adipocyte markers including *Ucp1*, *Dio2, Cox7a1, Cox8b,* and *Cidea,* as well as transcriptional regulators including *PPARa*, *C/EBPb*, *Prdm16*, and *Pgc-1a*, was significantly higher in tAT than in iWAT but lower than in BAT (Fig. 1, *C* and *D*). Of note, whereas the adipocyte master regulators *PPARg1* and *PPARg2* were comparable in all four examined fat depots, the expression of white adipocyte-enriched genes including *Adipsin*, *Leptin*, *Resistin*, and *Adiponectin* was higher in tAT than in BAT, but lower than in iWAT and eWAT (Fig. 1*E*). Furthermore, in cultured fat explants, tAT responded to forskolin by inducing brown adipocyte genes; their expression levels in tAT were higher overall than in iWAT, and lower than in BAT (Fig. S1). Thus, the gene expression signature of tAT is intermediate between that of iWAT and BAT, indicating that tAT is a more natural beige fat than iWAT.

tAT is distinct from iWAT

Because tAT is anatomically adjacent to iWAT, we employed a simple model to determine whether it is part of iWAT or is a distinct depot. In lactating female mice, the axillary and inguinal WAT, two prototypical subcutaneous depots, were almost entirely replaced by hypertrophic mammary glands, whereas tAT did not undergo this change- it retained its beige color without any expansion during lactation (Fig. 2*A*). Histological analyses supported this observation. The ducts and alveolar lumina of the lactating glands expanded vastly into the iWAT and axillary WAT (Fig. 2*B*). This morphological change was also observed in the interscapular WAT of the anterior subcutaneous depot, although the adjacent interscapular BAT maintained its composition of multilocular brown adipocytes. In contrast to iWAT, tAT displayed a regular WAT morphology with the presence of a few smaller, multilocular adipocytes but a clear absence of lactating glands (Fig. 2*B*). Therefore, tAT is functionally distinct from iWAT and other subcutaneous depots.

Indeed, tAT is covered by a muscular septum that separates it from iWAT, which raises the possibility that it may be an intramuscular adipose tissue depot. To address this possibility, we performed trichrome staining of tAT and the surrounding thigh muscle (Fig. 2*C*). A thin collagen layer was clearly observed at the interface between iWAT and tAT, indicating that, whereas tAT is attached to the thigh muscle, it is not intramuscular fat (27). These data support that tAT is indeed a separate beige depot and thus has unique features atypical of regular white fat.

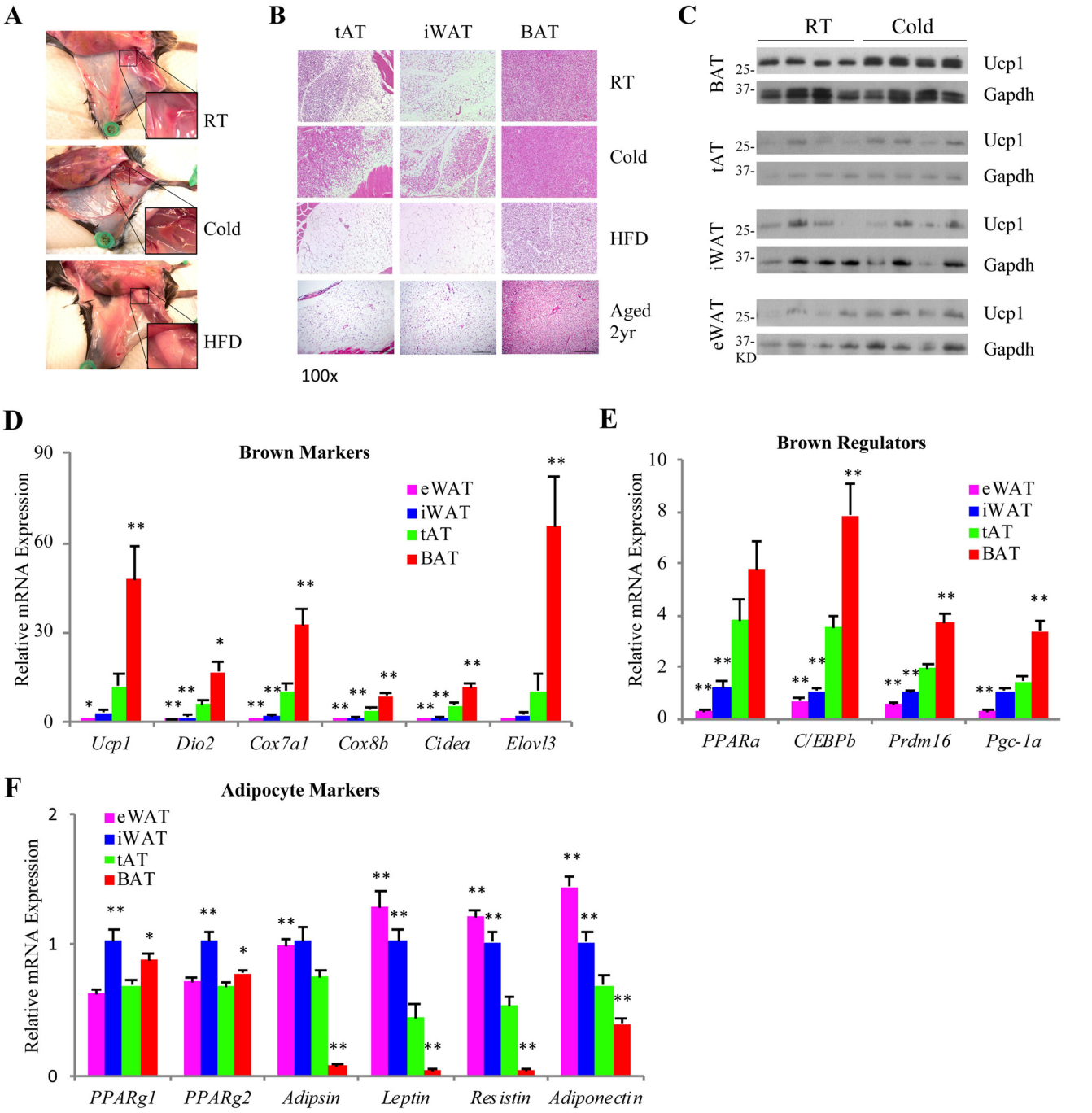

Figure 1. Thigh adipose tissue has dramatic browning potential. *A* and *B*, 6-week-old male C57B/6J mice were maintained at room temperature (*RT*) or exposed to 4 °C (*cold*) or placed on HFD for 3 weeks. *A*, anatomy of tAT. *B*, representative H&E staining of tAT, iWAT, and BAT under each condition (×100). *C*, Western blot analysis of UCP1 induction (UCP1 Rabbit Polyclonal antibody, Proteintech number 23673) by chronic cold exposure in four depots. C57B/6J mice were placed at 4 °C for 4 days and fat tissues were harvested to extract total proteins. Please note due to the smaller size of tAT, less protein was loaded for SDS-PAGE. *D–F*, during chronic cold challenge, relative mRNA expression of the indicated clusters of genes in four fat depots. Tissues were collected from 8-week-old male C57B/6J mice housed at 4 °C for 4 days. The gene expression levels were normalized to iWAT. *, $p < 0.05$; **, $p < 0.01$ *versus* tAT, $n = 9$ in each group.

Thiazolidinedione (TZD) induces pronounced brown remodeling of hypertrophic tAT in obesity

Having determined that tAT could easily be remodeled into beige fat, we subsequently investigated how tAT responds to obesity. We induced obesity via HFD feeding, upon which tAT cells adopted white adipocyte morphology as confirmed by the similar histological appearances of tAT and iWAT (Fig. 3*A*). This eliminated the possibility that tAT is a mixture of both brown and white adipocytes, and ensured that the depot was completely white prior to subsequent treatment. It has been shown that insulin-sensitizing reagents known as TZDs are capable of inducing the browning of white adipocytes *in vitro* and *in vivo* by activating PPARγ (10, 28). We therefore compared the brown remodeling of tAT induced by TZD treatment to that of canonical WAT. After a 5-week treatment with the TZD rosiglitazone, a greater number of smaller adipocytes

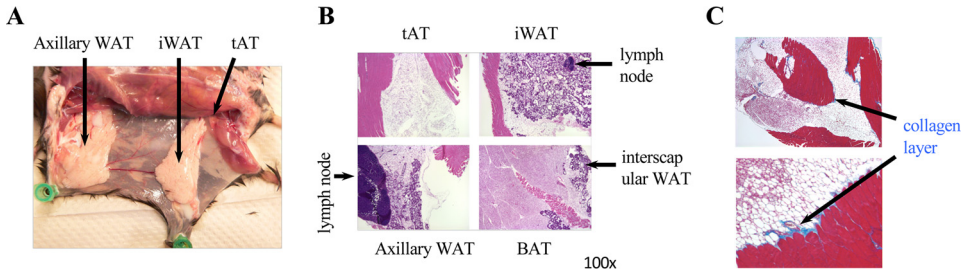

Figure 2. tAT is a distinct fat depot. *A,* overview of three fat depots as indicated from a lactating female. *B,* H&E staining of four different fat depots from lactating female. *C,* trichrome staining of the collagen layer (*light blue color*) between tAT and surrounding muscle.

appeared in tAT than in iWAT, in contrast to the expected lipid deposition in BAT (Fig. 3*A*). Strikingly, whereas tAT maintained a white adipocyte morphology on HFD, gene expression analysis revealed that tAT, compared with iWAT, exhibited over 2,600-fold higher expression of *Ucp1* (Fig. 3*B*) as well as much higher expression levels of other brown markers including *Cidea*, *Cox7a1*, and *Cox8b* (Fig. 3*B*). Notably, even though BAT-selective markers were expressed at much higher levels in tAT than in iWAT at the basal condition, they were still able to be induced by rosiglitazone treatment comparably in tAT and iWAT, unlike the blunted response observed in BAT (Fig. 3*B*). Furthermore, white adipocyte-enriched genes including *Adipsin*, *Leptin*, and *Resistin were* significantly repressed by rosiglitazone, whereas *Adiponectin* was mildly up-regulated (Fig. 3*C*). These data collectively illustrate that tAT is a hyperplastic fat depot that responds to pharmaceutical agents such as TZDs, in addition to physiological manipulations such as cold exposure and diet. qPCR analysis was also performed for classically-studied regulators of BAT-mediated thermogenesis. Surprisingly, little to no change was observed in the expression of *C/EBPb, Prdm16, PGC-1a,* and *Hoxc10* (29) in tAT after rosiglitazone treatment (Fig. 3*D*), suggesting that the browning capacity of tAT may be regulated through other means.

Global transcriptome revealed tAT as a distinct fat depot

To characterize the "natural" beige state of tAT from a molecular perspective, we performed single-end RNA-seq of poly(A)-selected RNAs from tAT and three other well-defined adipose depots (BAT, eWAT, and iWAT) in diet-induced obesity (DIO) mice. Under DIO, tAT exhibited a WAT morphology and a more pronounced difference compared with iWAT than under cold exposure (Table S1). Sequenced reads were aligned against mouse Ensembl gene annotations (mm10) using TopHat and quantified using Cufflinks (30). We first set out to provide a quantitative global transcriptomic proximity of tAT with the three classical adipose tissues by using expression levels of annotated protein-coding genes to calculate all possible pairwise correlations among the 16 samples (Fig. 4*A*). Compared with the correlations between classical BAT and WAT (iWAT and eWAT), which are highly divergent in morphology and physiology ($r = 0.5–0.7$), tAT samples showed a consistent and higher correlation with both WAT ($r = 0.75–0.94$) and BAT ($r = 0.74–0.88$) groups. Furthermore, hierarchical clustering (Fig. S2) and principal component analysis (Fig. 4*B*) revealed that whereas BAT samples were primarily discriminated from the rest, tAT samples displayed a tight and distinct cluster from eWAT and iWAT samples. Taken together, the global projection of the transcriptome strongly suggests that tAT is a distinct fat depot with molecular features that are intermediate between those of BAT and WAT.

tAT exhibits BAT-like properties

We then attempted to discover a plausible biological role of this new fat depot by identifying the significantly differentially expressed protein-coding genes (DEGs) with respect to BAT, eWAT, and iWAT (Fig. S3). As expected, the comparisons between BAT and eWAT (2,674 genes) or iWAT (2,311 genes) yielded a large number of DEGs, whereas the smallest change was observed between eWAT and iWAT (114 genes). Interestingly, the number of DEGs between BAT and tAT (1,271) was about half the number of DEGs between BAT and WAT (Fig. S3), suggesting that there is greater transcriptomic proximity between tAT and BAT than between BAT and WATs.

We proceeded to investigate the specific set of DEGs in tAT *versus* classical WAT. We detected 116 and 48 up-regulated protein-coding genes in tAT compared with eWAT and iWAT, respectively (fold-change ≥ 3, $q < 0.01$) (Fig. 5*A*, Fig. S3), both of which were enriched for highly similar categories of gene ontologies such as "single-organism catabolic process" and "carboxylic acid metabolic process" (Fig. S4, *A* and *C*). Of these, as many as 40 genes ($p < 2.2e-16$, hypergeometric test) (Fig. 5*A*), including key brown fat markers such as *Ucp1* and *PPARα* (Fig. 5*E*), were found to be commonly up-regulated in tAT. These genes showed functional specialization associated with fatty acid oxidation and fatty acid metabolism (Fig. 5*C*), thereby suggesting a possible role of energy expenditure in tAT.

A parallel analysis of the down-regulated DEGs in tAT compared with eWAT or iWAT identified 673 and 155 genes, respectively, with 134 common ones ($p < 2.2e-16$, hypergeometric test) (Fig. 5*B*, Fig. S3). Independent gene ontologies performed on these three gene lists (673, 155, and 134 genes) showed a high degree of overlap in the enriched processes mostly related to immune and inflammatory responses (Fig. 5*D*, Fig. S4, *B* and *D*), indicating a repressed inflammatory gene program in tAT.

Because the GO analysis of the regulated genes in tAT with respect to WAT suggests that tAT manifests BAT-like properties (Fig. 5, *C* and *D*), we integrated the gene expression profiles of BAT to determine whether tAT and BAT exhibit similar gene expression patterns relative to WATs. Remarkably, BAT and tAT shared consistent expression trends, and the extent of

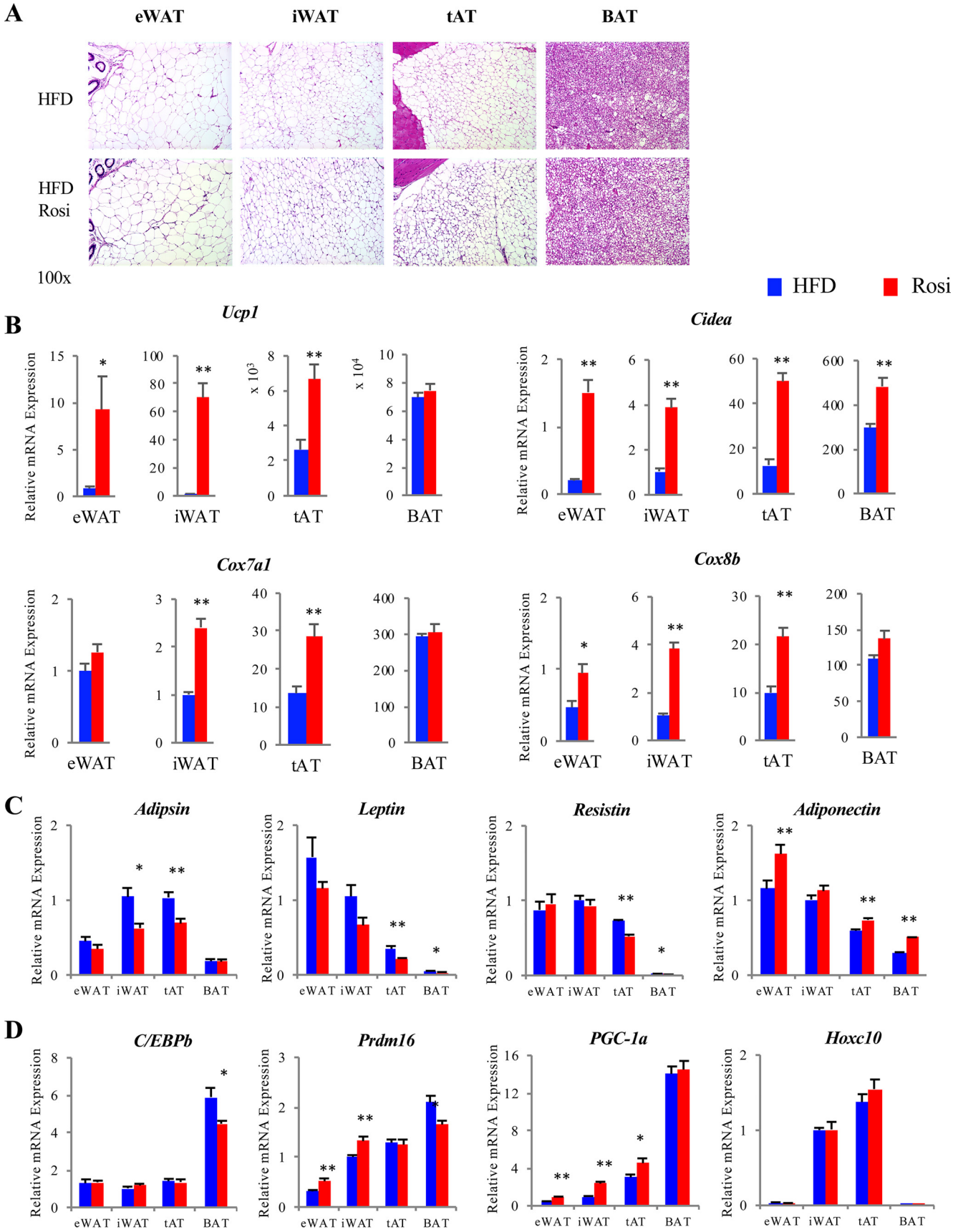

Figure 3. Thigh adipose tissue has WAT character and remains responsive to TZD-induced remodeling. 9-Week-old male C57B/6J mice were placed on HFD for 4 weeks and then treated with rosiglitazone (*Rosi*) for 5 weeks. Mice were sacrificed *ad libitum*. *A,* histology of four fat depots. *B–D,* qPCR analysis of gene expression in these four fat depots. *, $p < 0.05$; **, $p < 0.01$ for HFD *versus* Rosi within the same fat depot, $n = 6$.

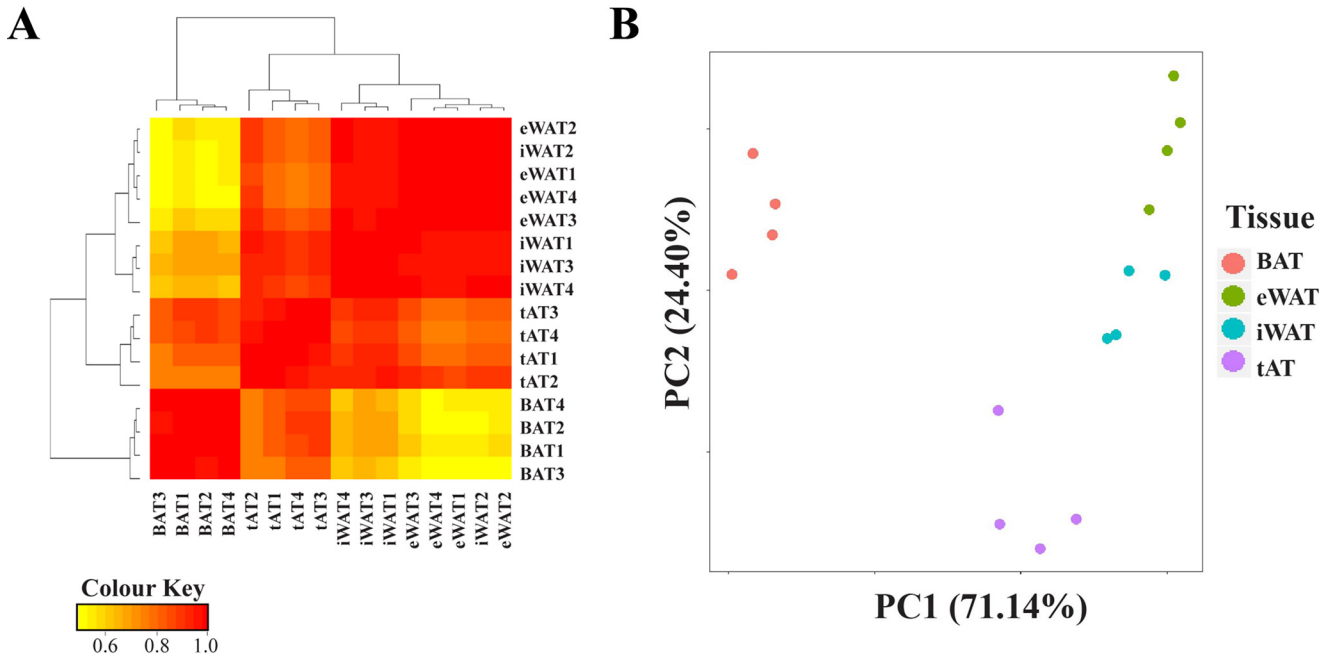

Figure 4. Global transcriptome landscape of BAT, eWAT, iWAT, and tAT. *A,* heat map of clustered correlation among the four depots. *B,* principal component analysis analysis on 10,347 protein coding genes with average FPKM ≥1 in all 4 adipose types in DIO mice.

expression change was more robust in BAT than in tAT (Fig. 5, *E–G*, Table S2).

Concordant global transcriptome difference of tAT and BAT with reference to WAT

To gain a deeper understanding of the similarity between BAT and tAT, we compared the dynamic of expression changes of BAT and tAT, each against eWAT (Fig. 6*A*) and iWAT (Fig. 6*B*). The scatterplot of global expression changes of BAT and tAT compared with eWAT displayed a strong positive linear correlation ($r = 0.71$, $p < 2.2e\text{-}16$), indicating that most genes shared the same direction of regulation in tAT and BAT compared with eWAT (Fig. 6*A*). A similar positive correlation was also observed when BAT and tAT were compared with iWAT ($r = 0.64$, $p < 2.2e\text{-}16$) (Fig. 6*B*). In parallel, tAT and iWAT were distinguished by comparing their dynamic of expression changes against eWAT (Fig. 6*C*) and BAT (Fig. 6*D*), respectively. Indeed, the magnitude of differences between tAT and eWAT was larger than that between iWAT and eWAT, as evidenced by most points lying above $y = x$ (line not plotted) and the regression line (Fig. 6*C*). In contrast, for the scatterplot for tAT/BAT *versus* iWAT/BAT, the latter showed a greater magnitude of differences than the former, again with the majority of points lying below $y = x$ and the generated regression line (Fig. 6*D*). We further pursued this finding by comparing the identities of the genes that showed the same direction of regulation in BAT and tAT, when compared with the same WAT type (Fig. 6, *E–H*). In all four categories, it was apparent that tAT showed a smaller number of DEGs compared with BAT, due to the greater transcriptomic proximity between tAT and WAT than between iWAT/eWAT and BAT (Fig. 6, *A* and *B*). Nonetheless, the overlaps of the genes were significant in all cases ($p < 2.2e\text{-}16$, hypergeometric test), which indicates that tAT exhibits a global resemblance to BAT in diet-induced obesity.

PPARα is dispensable for the brown character of tAT

PPARα plays key roles in regulating fatty acid oxidation and mitochondrial biogenesis. Among the brown adipocyte genes enriched in tAT, it was one of the few transcription factors (Fig. 5*E*). Interestingly, unlike other thermogenic regulators (Fig. 3*D*), *PPARα* was induced by rosiglitazone treatment across all four fat depots examined (Fig. 7*A*), suggesting a potential role in regulating adipose browning. We further investigated the effects of PPARα on tAT *in vivo*. In *ad libitum* chow-fed mice sacrificed at room temperature, the morphologies of eWAT, iWAT, tAT, and BAT were indistinguishable between Ppara$^{-/-}$ and WT mice (Fig. 7*B*). Likewise, there was no significant difference in the expression of brown markers, inflammatory markers, and white adipocyte markers in any of the white depots in the Ppara$^{-/-}$ mice compared with the WT mice (Fig. 7, *C–E*). Furthermore, in line with a recent finding of the dispensable role of PPARα in cold-induced adipose browning (31), there was no effect of PPARα knockout on the brown remodeling of tAT or iWAT upon cold challenge (data not shown). Ablation of PPARα also had minimal effect on adipogenesis and brown gene expression in tAT-derived adipocyte progenitors (Fig. S5). Therefore, PPARα is unlikely to account for the brown character of tAT.

Discussion

The current study indicates that tAT is hyperplastic and has a dramatic browning potential, as observed through its significantly higher expression of brown fat markers than iWAT. Its unique gene expression profile supports a classification as a beige adipose depot distinct from both iWAT and BAT, which was further confirmed by analysis of fat tissues from lactating mice. Upon high-fat diet feeding and subsequent rosiglitazone treatment, brown gene expression was significantly higher in

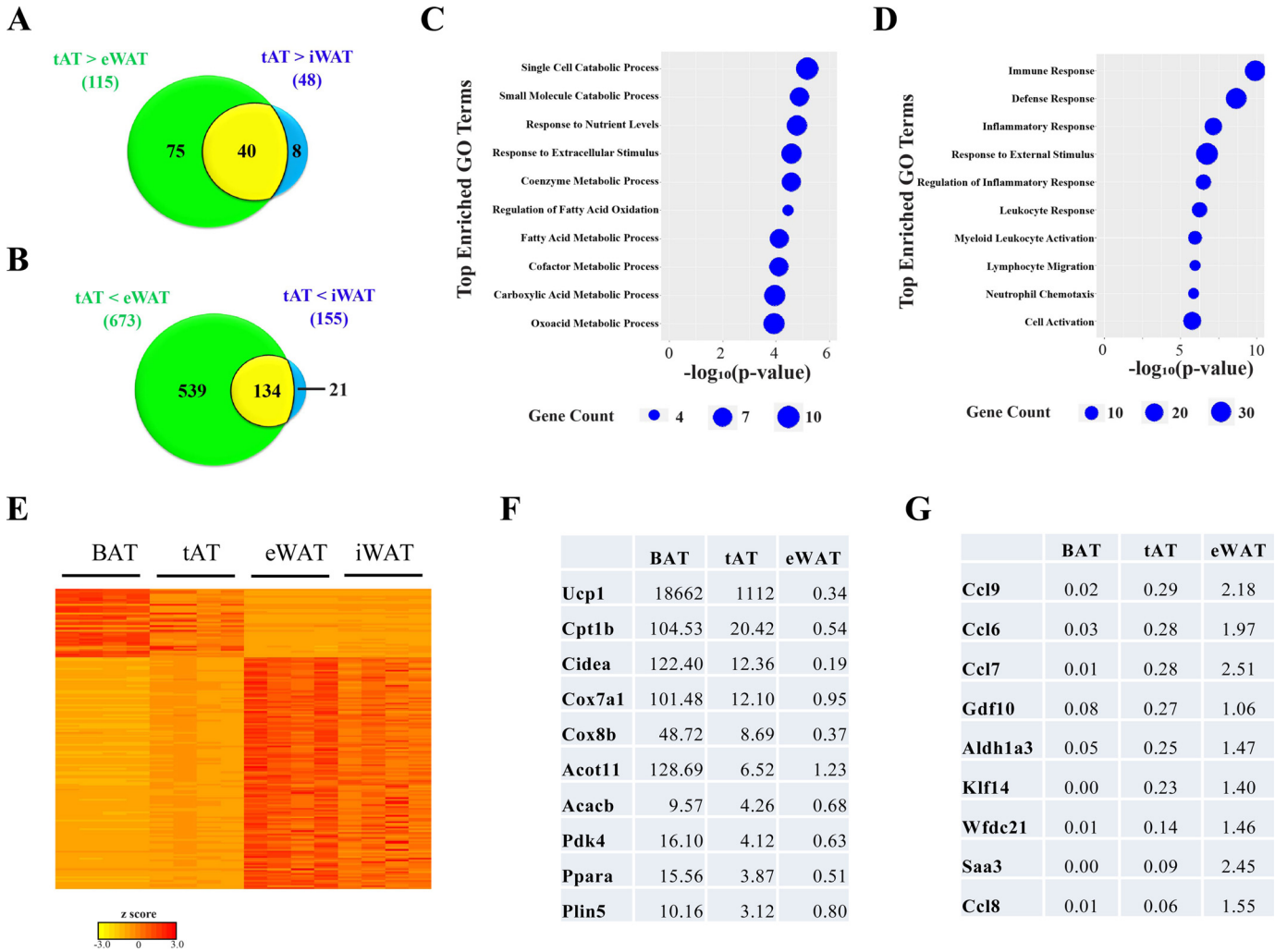

F

	BAT	tAT	eWAT
Ucp1	18662	1112	0.34
Cpt1b	104.53	20.42	0.54
Cidea	122.40	12.36	0.19
Cox7a1	101.48	12.10	0.95
Cox8b	48.72	8.69	0.37
Acot11	128.69	6.52	1.23
Acacb	9.57	4.26	0.68
Pdk4	16.10	4.12	0.63
Ppara	15.56	3.87	0.51
Plin5	10.16	3.12	0.80

G

	BAT	tAT	eWAT
Ccl9	0.02	0.29	2.18
Ccl6	0.03	0.28	1.97
Ccl7	0.01	0.28	2.51
Gdf10	0.08	0.27	1.06
Aldh1a3	0.05	0.25	1.47
Klf14	0.00	0.23	1.40
Wfdc21	0.01	0.14	1.46
Saa3	0.00	0.09	2.45
Ccl8	0.01	0.06	1.55

Figure 5. tAT exhibits BAT-like properties. *A* and *B*, Venn diagrams comparing the overlaps of significantly (*A*) up-regulated and (*B*) down-regulated protein-coding genes in tAT with respect to eWAT and iWAT. *C*, top 10 enriched gene ontology terms for 40 protein-coding genes that are significantly higher expressed in tAT than both eWAT and iWAT. Size of the bubble is proportional to the number of genes for each enriched GO term. *D*, top 10 enriched gene ontology terms for 134 protein-coding genes that are significantly lower expressed in tAT than both eWAT and iWAT. *E*, heat map depicting the expression profile differences of all four adipose types using 40 up- and 134 common significantly down-regulated genes in tAT compared with both iWAT and eWAT identified in *A* and *B*. The full gene list is in Table S2. *F* and *G*, representative up-regulated (*F*) and down-regulated (*G*) genes in tAT from the heat map in *E*.

tAT than in iWAT, suggesting that tAT is a metabolically healthier depot with greater browning capacity. RNA-Seq revealed an up-regulation of genes involved in fatty acid metabolism pathways and down-regulation of genes involved in inflammatory processes. Mouse adipose tissues are generally classified as BAT, WAT, or beige/brite depots (24–26). Because of its much higher expression of brown adipocyte genes, tAT is distinct from the canonical beige depots, such as the suprascapular, anterior subcutaneous, and inguinal depots (*e.g.* Ucp1 >2600-fold of iWAT in DIO; >10-fold of iWAT ≈ suprascapular ≈ anterior subcutaneous under cold challenge (24)). Its fully-white adipose morphology in DIO or aging rules out the possibility that it is a mixture of brown adipocytes and white adipocytes (27). Therefore, we conclude that tAT is a unique, natural beige fat depot.

The hyperplasticity of tAT suggests that this depot serves as a more suitable model for studies of adipose plasticity than the traditionally used inguinal WAT. Given its higher basal expression of brown markers, further characterization of tAT may allow us to identify potential targets to augment the plasticity of other adipose tissues including eWAT and iWAT, and to pinpoint the factors involved in maintaining metabolic homeostasis. The hyperplasticity of tAT is likely governed by synergistic factors, such as both catabolic regulators and anti-inflammatory factors, rather than a single one. Intriguingly, our analysis of brown adipocyte markers revealed that tAT exhibits over 2,600-fold higher expression of *Ucp1* than iWAT does on HFD and activates the fatty acid oxidation pathway, yet still maintains a white adipocyte morphology. The mechanism by which white adipocytes sustain such high metabolic rate has yet to be elucidated. Moreover, despite this hyper-catabolic state, tAT exhibits a decrease in inflammation. This anti-inflammatory mechanism in tAT may be crucial toward targeting insulin resistance associated with obesity.

PPARα seemed to perfectly underlie the activation of fatty acid oxidation and repression of inflammation observed in tAT due to its expression pattern and its well-established functions (32). To our surprise, it appears to be dispensable for the beige

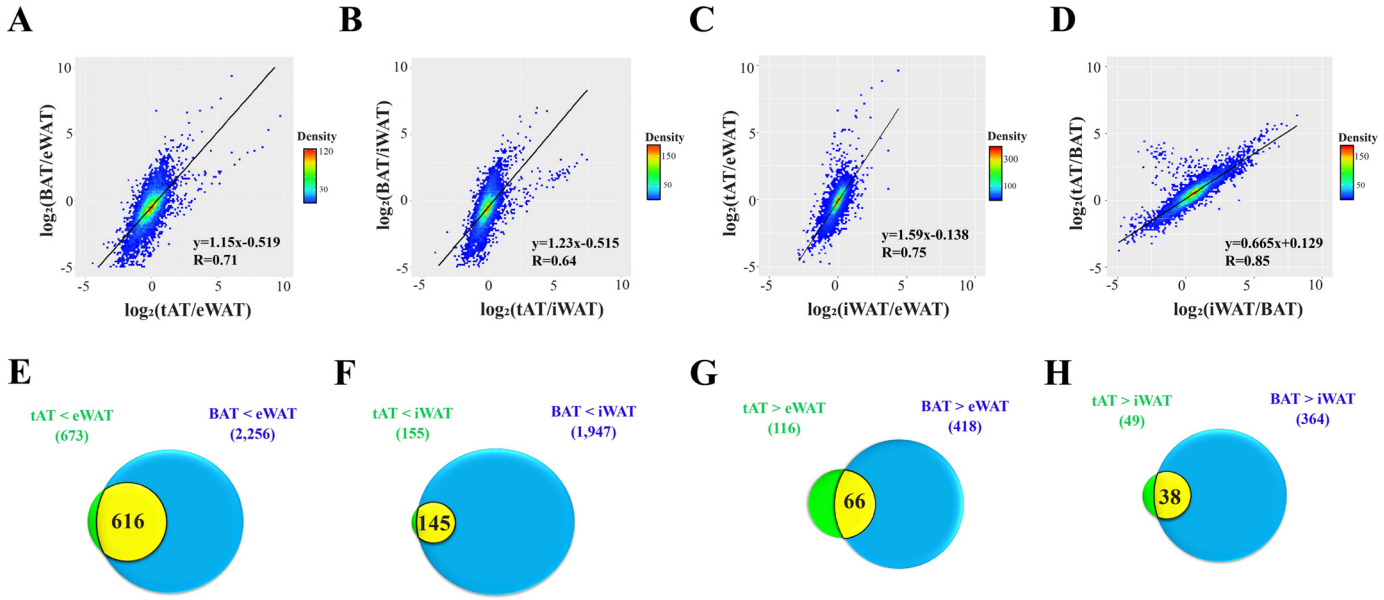

Figure 6. Concordant global transcriptome difference of tAT and BAT with reference to WAT. *A–D,* Hexbin density plot depicting the correlation of global expression differences between the indicated depots. *A,* BAT and tAT with respect to eWAT, and 10,368 genes have been included in the analysis; *B,* BAT and tAT with respect to iWAT, and 10,431 genes have been included in the analysis; *C,* tAT and iWAT with respect to eWAT, and 11,382 genes have been included in the analysis; *D,* tAT and iWAT with respect to BAT, and 10,431 have been included in the analysis. Genes with average FPKM ≥1 in 4 depots have been included in the analysis, and density of the gene counts are represented by different color scales. *E* and *F,* Venn diagrams comparing the overlaps of significantly down-regulated genes in tAT and BAT with respect to (*E*) eWAT and (*F*) iWAT. *G* and *H,* Venn diagrams comparing the overlaps of significantly down-regulated genes in tAT and BAT with respect to (*G*) eWAT and (*H*) iWAT.

features of tAT as demonstrated in *PPARa*$^{-/-}$ mice exposed to ambient temperature or cold challenge. These mice not only have normal BAT function (33, 34), but also have intact browning capacity in inguinal fat (31). A possible explanation is compensation from PPARγ. It has been shown that PPARγ and its downstream targets CD36 and aP2 are induced in the liver of *PPARa*$^{-/-}$ mice (35), and the expression of PPARγ and aP2 is overall normal in *PPARa*$^{-/-}$ mice (Fig. 7, Fig. S5) (31). Functionally, PPARγ and PPARα overlap as they both regulate lipid metabolism, promote mitochondrial biogenesis and activity, and repress inflammation (36, 37). The interplay between PPARγ and PPARα is worthy of further investigation.

Beige adipocytes are believed to arise from a smooth muscle-like lineage (38), which is possibly the case for tAT as well, although further lineage-tracing studies are necessary for a more definitive answer. This raises the question of why tAT adipocytes from the same lineage as beige adipocytes would show a marked enhancement of browning capability. The most probable reason is environment-based: tAT is adjacent to muscle and is thus supplied with more nutrients and oxygen, as well as neuronal input. The precise function of tAT in mice is unclear. Due to its small size, it is unlikely to affect whole body metabolism. However, it may serve as a sensor of environmental change because of its hyperplasticity. Given its proximity to muscle, it is also likely to be sensitive to exercise-induced brown remodeling. In either case, we speculate that tAT releases signals to the rest of the body to direct the metabolic function of other organs such as larger adipose depots or the liver. Another possibility is that tAT functions as a cushion surrounding the synovial joint between the femur and pelvis, perhaps maintaining a homeostatic temperature of the joint for movement or blood flow.

The identification of this intrinsically-beige adipose depot in mice has numerous implications in the field of metabolic diseases and their treatments. tAT may be more representative of human thermogenic adipose tissue than inducible beige cells derived from iWAT due to its greater capacity for browning (24). As such, its molecular profile underlying its hyperplasticity may provide key insights into the factors that promote a more favorable energy balance via increased energy expenditure. This would yield a paradigm shift in our understanding of beige adipocytes as well as in current approaches toward brown remodeling of white fat in diabetes and obesity therapeutics.

Experimental procedures

Animal studies

Animals were housed and cared for within the procedures approved by the Columbia University Animal Care and Utilization Committee. WT and *Pparα* knockout mice on a C57BL/6J background were obtained from Jackson Laboratories. Mice were housed on a 12-h light/dark cycle with access to regular chow (Pico Lab Diet 5053, Purina Mill Inc., Brentwood, MO) and water *ad libitum*. For chronic cold exposure, mice were housed at 4 °C for 4 days. To promote DIO, animals were fed a HFD, of which 60% of the calories were obtained from fat, 20% from carbohydrates, and 20% from protein (D12492, Research Diets Inc., New Brunswick, NJ). Rosiglitazone treatment was administered as an admixture of Avandia (ab142461, Abcam) and the HFD at a dose of 5 mg/kg of body weight.

tAT stromal vascular fraction (SVF) cell isolation and differentiation

tAT fat pads from ~10 control or Pparα knockout mice at 4 weeks of age were pooled and minced, then digested with 0.2%

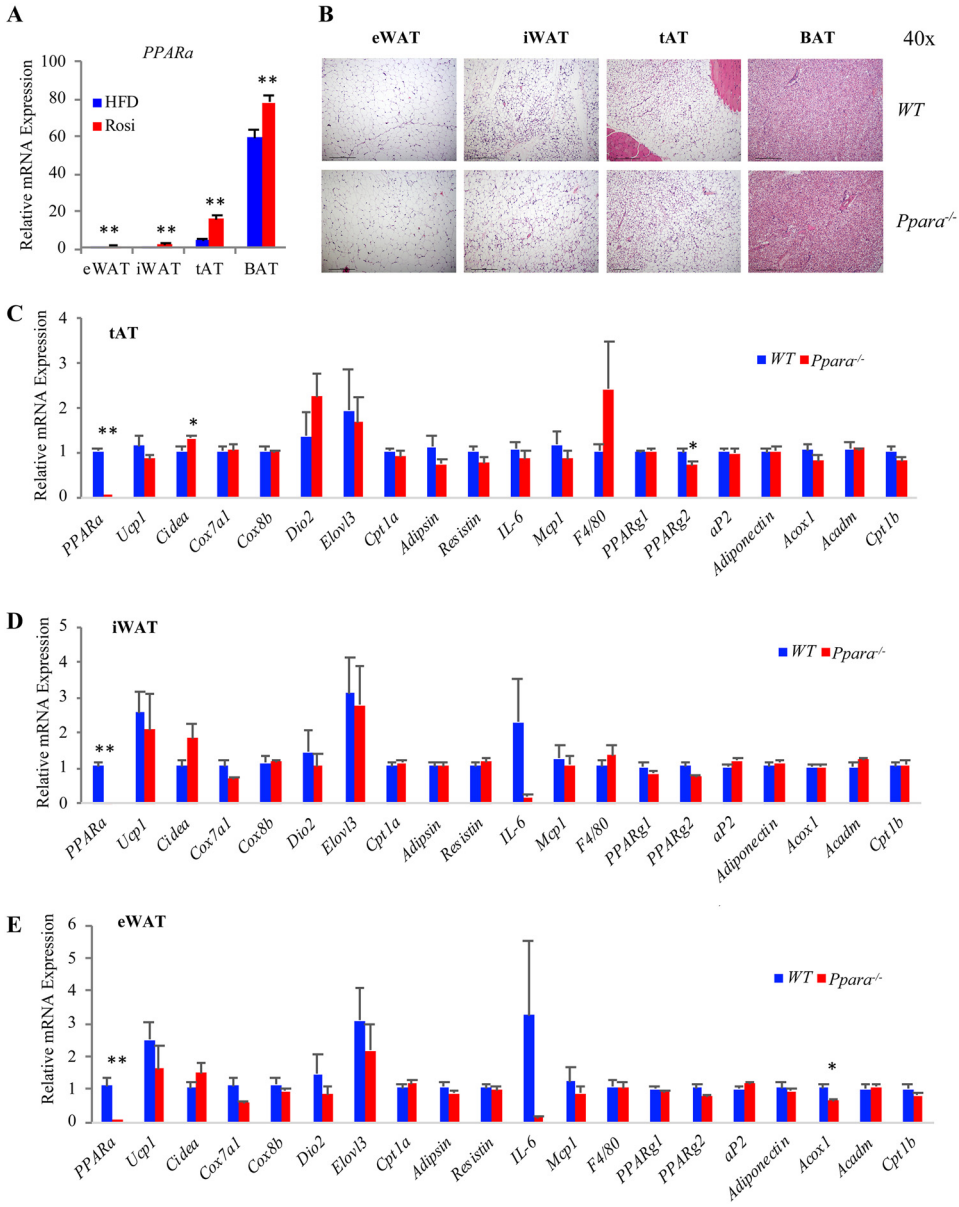

Figure 7. PPARα is dispensable for browning features of tAT. *A,* gene expression levels of PPARα in fat depots from rosiglitazone- and HFD-treated mice. *B,* H&E staining of adipose tissues from WT and *PPARa*$^{-/-}$ mice housed at ambient temperature (×40). *C–E,* relative mRNA expression levels of the indicated genes in WT *versus* Ppara$^{-/-}$ mice in tAT, iWAT, and eWAT. *, $p < 0.05$; **, $p < 0.01$ *versus* WT within the same depot, $n = 6$.

collagenase for 30 min at 37 °C on an orbital shaker at 500 rpm. The digested tissue was passed through a 70-μm cell strainer and centrifuged at 1500 rpm for 5 min to pellet SVF cells. The cells were then cultured and expanded in Dulbecco's modified Eagle's medium supplemented with 10% fetal bovine serum and gentamycin. Upon confluence after 2 days, the SVF cells were induced to undergo adipogenesis by adding 850 nM insulin, 0.5 μM dexamethasone, and 250 μM 3-isobutyl-1-methylxanthine for 3 days, and were then maintained in Dulbecco's modified Eagle's medium with 10% fetal bovine serum and 210 nM insulin until fully differentiated for analysis.

RNA analysis

Whole tissues were dissected from one side of each mouse and homogenized in TRI Reagent (Sigma). Total RNA was isolated using the NucleoSpin RNA set kit (Macherey-Nagel) following the manufacturer's protocol. 1 μg of RNA was used for reverse transcription into cDNA with the High Capacity cDNA Kit (Applied Biosystems) according to the manufacturer's instructions. Real-time PCR (qPCR) was then performed using GoTaq qPCR master mix (Promega). Relative gene expression levels for all tissues were calculated using the $\Delta\Delta C_t$ method, with *RPL23* as an internal control.

RNA-seq data analysis

Sequencing reads were first mapped to the mouse reference genome (mm10) using TopHat-2.0.9 (30) alignment tool and subsequently quantified into FPKM units using Cufflinks-2.1.1 (30). Differential expression analysis was then performed using the Cuffdiff program, found within the Cufflinks package. Within each pairwise comparison, genes were considered significantly differentially expressed when (i) average FPKM ≥1 in

at least one group, (ii) fold change ≥3, (iii) q-value <0.01, and (iv) maximum FPKM of the lower expressed group is at least 1 FPKM unit lower than the minimum FPKM of the higher expressed group. Gene set enrichment analysis was performed using DAVID Bioinformatics Resources 6.8 (39, 40) and only Biological Process and Molecular Function terms (GOTERM_BP_FAT and GOTERM_MF_FAT) were considered. Heat maps and all other plots were generated using R. The RNA-seq data are deposited in NCBI's Gene Expression Omnibus database (GEO GSE123511).

Histology

Fat tissues were fixed in 10% buffered formalin and embedded in paraffin wax. The paraffin-embedded tissues were sectioned to a thickness of ~5 μm. Tissues were then stained with hematoxylin and eosin (H&E), and, where necessary, trichrome was applied to stain for collagen to examine tissue morphology.

Statistical analysis

GraphPad Prism 6 (GraphPad Software) was used for all analyses and statistical significance was determined at $p < 0.05$. All data points are presented as mean ± S.E. One-way analysis of variance followed by Tukey post-hoc test was utilized for multiple comparisons.

Author contributions—M. C., J. Y., and L. Q. data curation; M. C., Y. C. L., and M. N. writing-original draft; Y. C. L. and J. Y. formal analysis; Y. C. L., M. N., L. L., and L. Q. methodology; L. Q. conceptualization; L. Q. resources; L. Q. supervision; L. Q. funding acquisition; L. Q. investigation; L. Q. project administration; L. Q. writing-review and editing.

References

1. Zechner, R., Zimmermann, R., Eichmann, T. O., Kohlwein, S. D., Haemmerle, G., Lass, A., and Madeo, F. (2012) Fat signals: lipases and lipolysis in lipid metabolism and signaling. *Cell Metab.* **15,** 279–291 CrossRef Medline
2. Scherer, P. E. (2006) Adipose tissue: from lipid storage compartment to endocrine organ. *Diabetes* **55,** 1537–1545 CrossRef Medline
3. Trujillo, M. E., and Scherer, P. E. (2006) Adipose tissue-derived factors: impact on health and disease. *Endocr. Rev.* **27,** 762–778 CrossRef Medline
4. Cannon, B., and Nedergaard, J. (2004) Brown adipose tissue: function and physiological significance. *Physiol. Rev.* **84,** 277–359 CrossRef Medline
5. Ikeda, K., Maretich, P., and Kajimura, S. (2018) The common and distinct features of brown and beige adipocytes. *Trends Endocrinol. Metab.* **29,** 191–200 CrossRef Medline
6. Wu, J., Cohen, P., and Spiegelman, B. M. (2013) Adaptive thermogenesis in adipocytes: is beige the new brown? *Genes Dev.* **27,** 234–250 CrossRef Medline
7. Vitali, A., Murano, I., Zingaretti, M. C., Frontini, A., Ricquier, D., and Cinti, S. (2012) The adipose organ of obesity-prone C57BL/6J mice is composed of mixed white and brown adipocytes. *J. Lipid Res.* **53,** 619–629 CrossRef Medline
8. Cousin, B., Cinti, S., Morroni, M., Raimbault, S., Ricquier, D., Pénicaud, L., Pénicaud, L., and Casteilla, L. (1992) Occurrence of brown adipocytes in rat white adipose tissue: molecular and morphological characterization. *J. Cell Sci.* **103,** 931–942 Medline
9. Himms-Hagen, J., Cui, J., Danforth, E., Jr., Taatjes, D. J., Lang, S. S., Waters, B. L., and Claus, T. H. (1994) Effect of CL-316,243, a thermogenic β3-agonist, on energy balance and brown and white adipose tissues in rats. *Am. J. Physiol.* **266,** R1371–R1382 Medline
10. Qiang, L., Wang, L., Kon, N., Zhao, W., Lee, S., Zhang, Y., Rosenbaum, M., Zhao, Y., Gu, W., Farmer, S. R., and Accili, D. (2012) Brown remodeling of white adipose tissue by SirT1-dependent deacetylation of Pparγ. *Cell* **150,** 620–632 CrossRef Medline
11. Mulya, A., and Kirwan, J. P. (2016) Brown and beige adipose tissue: therapy for obesity and its comorbidities? *Endocrinol. Metab. Clin. North Am.* **45,** 605–6021 CrossRef Medline
12. Kajimura, S., Spiegelman, B. M., and Seale, P. (2015) Brown and beige fat: physiological roles beyond heat generation. *Cell Metab.* **22,** 546–559 CrossRef Medline
13. Barbatelli, G., Murano, I., Madsen, L., Hao, Q., Jimenez, M., Kristiansen, K., Giacobino, J. P., De Matteis, R., and Cinti, S. (2010) The emergence of cold-induced brown adipocytes in mouse white fat depots is determined predominantly by white to brown adipocyte transdifferentiation. *Am. J. Physiol. Endocrinol. Metab.* **298,** E1244–E1253 CrossRef Medline
14. Rosenwald, M., Perdikari, A., Rülicke, T., and Wolfrum, C. (2013) Bi-directional interconversion of brite and white adipocytes. *Nat. Cell Biol.* **15,** 659–667 CrossRef Medline
15. Wang, Q. A., Tao, C., Gupta, R. K., and Scherer, P. E. (2013) Tracking adipogenesis during white adipose tissue development, expansion and regeneration. *Nat. Med.* **19,** 1338–1344 CrossRef Medline
16. Harms, M., and Seale, P. (2013) Brown and beige fat: development, function and therapeutic potential. *Nat. Med.* **19,** 1252–1263 CrossRef Medline
17. Virtanen, K. A., Lidell, M. E., Orava, J., Heglind, M., Westergren, R., Niemi, T., Taittonen, M., Laine, J., Savisto, N. J., Enerbäck, S., and Nuutila, P. (2009) Functional brown adipose tissue in healthy adults. *N. Engl. J. Med.* **360,** 1518–1525 CrossRef Medline
18. Sharp, L. Z., Shinoda, K., Ohno, H., Scheel, D. W., Tomoda, E., Ruiz, L., Hu, H., Wang, L., Pavlova, Z., Gilsanz, V., and Kajimura, S. (2012) Human BAT possesses molecular signatures that resemble beige/brite cells. *PLoS ONE* **7,** e49452 CrossRef Medline
19. Lidell, M. E., Betz, M. J., Dahlqvist Leinhard, O., Heglind, M., Elander, L., Slawik, M., Nilsson, D., Romu, T., Nuutila, P., Virtanen, K. A., Beuschlein, F., Persson, A., Borga, M., and Enerbäck, S. (2013) Evidence for two types of brown adipose tissue in humans. *Nat. Med.* **19,** 631–634 CrossRef Medline
20. Shinoda, K., Luijten, I. H., Hasegawa, Y., Hong, H., Sonne, S. B., Kim, M., Xue, R., Chondronikola, M., Cypess, A. M., Tseng, Y. H., Nedergaard, J., Sidossis, L. S., and Kajimura, S. (2015) Genetic and functional characterization of clonally derived adult human brown adipocytes. *Nat. Med.* **21,** 389–394 CrossRef Medline
21. Poher, A. L., Altirriba, J., Veyrat-Durebex, C., and Rohner-Jeanrenaud, F. (2015) Brown adipose tissue activity as a target for the treatment of obesity/insulin resistance. *Front. Physiol.* **6,** 4 Medline
22. Farmer, S. R. (2009) Obesity: be cool, lose weight. *Nature* **458,** 839–840 CrossRef Medline
23. Seale, P., Conroe, H. M., Estall, J., Kajimura, S., Frontini, A., Ishibashi, J., Cohen, P., Cinti, S., Spiegelman, B. M. (2011) Prdm16 determines the thermogenic program of subcutaneous white adipose tissue in mice. *J. Clin. Invest.* **121,** 96–105 CrossRef Medline
24. Zhang, F., Hao, G., Shao, M., Nham, K., An, Y., Wang, Q., Zhum Y., Kusminski, C. M., Hassan, G., Gupta, R. K., Zhai, Q., Sun, X., Scherer, P. E., and Oz, O. K. (2018) An adipose tissue atlas: an image-guided identification of human-like BAT and beige depots in rodents. *Cell Metab.* **27,** 252–262.e3 CrossRef Medline
25. de Jong, J. M., Larsson, O., Cannon, B., and Nedergaard, J. (2015) A stringent validation of mouse adipose tissue identity markers. *Am. J. Physiol. Endocrinol. Metab.* **308,** E1085–E1105 CrossRef Medline
26. Waldén, T. B., Hansen, I. R., Timmons, J. A., Cannon, B., and Nedergaard, J. (2012) Recruited *vs.* nonrecruited molecular signatures of brown, "brite," and white adipose tissues. *Am. J. Physiol. Endocrinol. Metab.* **302,** E19–E31 CrossRef Medline
27. Almind, K., Manieri, M., Sivitz, W. I., Cinti, S., and Kahn, C. R. (2007) Ectopic brown adipose tissue in muscle provides a mechanism for differences in risk of metabolic syndrome in mice. *Proc. Natl. Acad. Sci. U.S.A.* **104,** 2366–2371 CrossRef Medline

28. Wang, H., Qiang, L., and Farmer, S. R. (2008) Identification of a domain within peroxisome proliferator-activated receptor γ regulating expression of a group of genes containing fibroblast growth factor 21 that are selectively repressed by SIRT1 in adipocytes. *Mol. Cell Biol.* **28,** 188–200 CrossRef Medline
29. Ferrannini, G., Namwanje, M., Fang, B., Damle, M., Li, D., Liu, Q., Lazar, M. A., and Qiang, L. (2016) Genetic backgrounds determine brown remodeling of white fat in rodents. *Mol. Metab.* **5,** 948–958 CrossRef Medline
30. Trapnell, C., Roberts, A., Goff, L., Pertea, G., Kim, D., Kelley, D. R., Pimentel, H., Salzberg, S. L., Rinn, J. L., and Pachter, L. (2012) Differential gene and transcript expression analysis of RNA-seq experiments with TopHat and Cufflinks. *Nat. Protoc.* **7,** 562–578 CrossRef Medline
31. Defour, M., Dijk, W., Ruppert, P., Nascimento, E. B. M., Schrauwen, P., and Kersten, S. (2018) The peroxisome proliferator-activated receptor α is dispensable for cold-induced adipose tissue browning in mice. *Mol. Metab.* **10,** 39–54 CrossRef Medline
32. Li, P., Zhu, Z., Lu, Y., and Granneman, J. G. (2005) Metabolic and cellular plasticity in white adipose tissue II: role of peroxisome proliferator-activated receptor-α. *Am. J. Physiol. Endocrinol. Metab.* **289,** E617–E626 CrossRef Medline
33. Xue, B., Coulter, A., Rim, J. S., Koza, R. A., and Kozak, L. P. (2005) Transcriptional synergy and the regulation of Ucp1 during brown adipocyte induction in white fat depots. *Mol. Cell Biol.* **25,** 8311–8322 CrossRef Medline
34. Kersten, S., Seydoux, J., Peters, J. M., Gonzalez, F. J., Desvergne, B., and Wahli, W. (1999) Peroxisome proliferator-activated receptor α mediates the adaptive response to fasting. *J. Clin. Invest.* **103,** 1489–1498 CrossRef Medline
35. Patsouris, D., Reddy, J. K., Müller, M., and Kersten, S. (2006) Peroxisome proliferator-activated receptor alpha mediates the effects of high-fat diet on hepatic gene expression. *Endocrinology* **147,** 1508–1516 CrossRef Medline
36. Varga, T., Czimmerer, Z., and Nagy, L. (2011) PPARs are a unique set of fatty acid regulated transcription factors controlling both lipid metabolism and inflammation. *Biochim. Biophys. Acta* **1812,** 1007–1022 CrossRef Medline
37. Tontonoz, P., and Spiegelman, B. M. (2008) Fat and beyond: the diverse biology of PPARγ. *Annu. Rev. Biochem.* **77,** 289–312 CrossRef Medline
38. Long, J. Z., Svensson, K. J., Tsai, L., Zeng, X., Roh, H. C., Kong, X., Rao, R. R., Lou, J., Lokurkar, I., Baur, W., Castellot, J. J., Jr., Rosen, E. D., and Spiegelman, B. M. (2014) A smooth muscle-like origin for beige adipocytes. *Cell Metab.* **19,** 810–820 CrossRef Medline
39. Huang da, W., Sherman, B. T., and Lempicki, R. A. (2009) Systematic and integrative analysis of large gene lists using DAVID bioinformatics resources. *Nat. Protoc.* **4,** 44–57 CrossRef Medline
40. Huang da, W., Sherman, B. T., and Lempicki, R. A. (2009) Bioinformatics enrichment tools: paths toward the comprehensive functional analysis of large gene lists. *Nucleic Acids Res.* **37,** 1–13 CrossRef Medline